5634–5650 *Nucleic Acids Research, 2018, Vol. 46, No. 11* *Published online 7 May 2018*
doi: 10.1093/nar/gky313

Flap endonuclease overexpression drives genome instability and DNA damage hypersensitivity in a PCNA-dependent manner

Jordan R. Becker[1], David Gallo[2,†], Wendy Leung[1,†], Taylor Croissant[1], Yee Mon Thu[1], Hai Dang Nguyen[1], Timothy K. Starr[3], Grant W. Brown[2] and Anja-Katrin Bielinsky[1,*]

[1]Department of Biochemistry, Molecular Biology, and Biophysics, University of Minnesota, Minneapolis, MN 55455, USA, [2]Department of Biochemistry and Donnelly Centre, University of Toronto, Toronto, ON M5S 3E2, Canada and [3]Department of Obstetrics, Gynecology, and Women's Health, University of Minnesota, Minneapolis, MN 55455, USA

Received December 13, 2017; Revised April 06, 2018; Editorial Decision April 09, 2018; Accepted April 16, 2018

ABSTRACT

Overexpression of the flap endonuclease FEN1 has been observed in a variety of cancer types and is a marker for poor prognosis. To better understand the cellular consequences of FEN1 overexpression we utilized a model of its *Saccharomyces cerevisiae* homolog, *RAD27*. In this system, we discovered that flap endonuclease overexpression impedes replication fork progression and leads to an accumulation of cells in mid-S phase. This was accompanied by increased phosphorylation of the checkpoint kinase Rad53 and histone H2A-S129. *RAD27* overexpressing cells were hypersensitive to treatment with DNA damaging agents, and defective in ubiquitinating the replication clamp proliferating cell nuclear antigen (PCNA) at lysine 164. These effects were reversed when the interaction between overexpressed Rad27 and PCNA was ablated, suggesting that the observed phenotypes were linked to problems in DNA replication. *RAD27* overexpressing cells also exhibited an unexpected dependence on the SUMO ligases *SIZ1* and *MMS21* for viability. Importantly, we found that overexpression of FEN1 in human cells also led to phosphorylation of CHK1, CHK2, RPA32 and histone H2AX, all markers of genome instability. Our data indicate that flap endonuclease overexpression is a driver of genome instability in yeast and human cells that impairs DNA replication in a manner dependent on its interaction with PCNA.

INTRODUCTION

Complete replication of the genome before cell division is a fundamental requirement for the multigenerational viability of all cellular organisms. Evolution has provided a highly conserved set of replication factors, which carry out an intricately coordinated array of activities. In the event of difficulty or error, a network of repair and checkpoint pathways has arisen to facilitate the completion of replication with a minimum of inheritable mutations. The high level of conservation in these replication-, repair- and checkpoint pathways has allowed us to utilize relatively simpler model organisms, such as *Saccharomyces cerevisiae*, to better understand how these processes are carried out in more complex metazoan systems. In this study, we started with the observation that the replication factor flap endonuclease 1 (FEN1) is frequently overexpressed in human cancer tissues and attempted to understand the effect that this has on DNA replication and genome stability in the simple organism *S. cerevisiae*.

FEN1 and its yeast homolog radiation sensitive 27 (*RAD27*) have a conserved function in DNA replication to process 5′ flaps, which are generated at the junction of Okazaki fragments on the lagging strand (1–3). Synthesis of the lagging strand is carried out primarily by polymerase (pol-) δ in conjunction with the homotrimeric replication clamp and processivity factor proliferating cell nuclear antigen (PCNA). Synthesis continues until the polymerase collides with the 5′ end of the preceding Okazaki fragment and displaces it into a 5′ flap (4). PCNA then coordinates the processing of this flap in a manner that is dependent on a conserved interaction between the PCNA interacting peptide (PIP) box of Rad27/FEN1 and the interdomain connector loop of PCNA (5–7). Flap cleavage results in a lig-

*To whom correspondence should be addressed. Tel: +1 612 624 2469; Fax: +1 612 624 0426; Email: bieli003@umn.edu
†The authors wish it to be known that, in their opinion, the second and third authors should be regarded as Joint Second Authors.
Present addresses:
Jordan R. Becker, Chromatin and Genome Integrity Laboratory, Wellcome Centre for Human Genetics, University of Oxford, Oxford OX3 7BN, UK.
Yee Mon Thu, Department of Biology, Grinnell College, Grinnell, IA 50112, USA.
Hai Dang Nguyen, Massachusetts General Hospital Cancer Center, Harvard Medical School, Charlestown, MA 02114, USA.

atable nick, which is sealed by DNA ligase I, completing Okazaki fragment maturation (4). In addition to its well described function in DNA replication, Rad27/FEN1 has also been implicated in 5′-deoxyribophosphate removal at abasic sites during base excision repair (BER) (8).

Deletion mutants of *RAD27* in yeast are viable but exhibit temperature sensitive growth, increased mutation rate, hyper-recombination, repeat tract instability and DNA damage sensitivity (9–12). Conversely, FEN1 overexpression has been observed in a wide variety of cancer types including gastric, prostate, testis, brain, lung, breast, ovarian and prostate and is a marker for poor prognosis (13–21). Despite the prevalence of overexpression in cancer, remarkably little is understood as to the effect of FEN1 overabundance on DNA replication, cell-cycle progression or genome stability. We hypothesized that overexpression of an enzyme capable of cleaving DNA strands that also interacts with PCNA and plays a crucial function in DNA replication could lead to negative effects on genome stability through the deregulation of any of these functions.

In addition to its coordinating role in unperturbed replication, PCNA is also subject to a number of post-translational modifications which endow it with the ability to coordinate cellular responses to replication stress (22). Ubiquitination of PCNA at the residue of lysine (K)164 by Rad6–Rad18 is an evolutionarily conserved response to replication stress triggered by persistent regions of replication protein A (RPA) coated single stranded (ss)DNA (23,24). This modification can activate two potential post-replicative repair (PRR) pathways dependent on the length of the ubiquitin chain (23). Mono-ubiquitin facilitates a switch from the processive replicative polymerases to specialized translesion polymerases that are able to tolerate replication over damaged DNA, albeit with an increased rate of nucleotide misincorporation (25). Alternatively, poly-ubiquitination facilitates an error-free template switching pathway of PRR capable of bypassing damaged sites and filling in ssDNA gaps (26). The mechanistic details of this pathway are not yet well understood. K164 is also a conserved target for attachment of a small ubiquitin-like modifier (SUMO). Unlike ubiquitination, this modification occurs during unperturbed S phase and serves to inhibit illegitimate recombination between nascent sister chromatids by recruiting the helicase/anti-recombinase suppressor of rad six 2 (Srs2) (27,28). Srs2 is thought to inhibit recombination at replication forks by disrupting the formation of Rad51 nucleoprotein filaments (29,30). Conversely, recent reports have pointed to a pro-recombination role for Srs2 that is independent of its interaction with PCNA (31,32).

In the present study, we have used an inducible overexpression system to modulate *RAD27* expression levels. Our findings indicate that overexpression causes marked impairment of DNA replication leading to delayed S phase progression and accumulation of DNA damage in a manner that is dependent on its interaction with PCNA. Unexpectedly, overexpression also dramatically increases DNA damage sensitivity that is linked to an inability to transfer ubiquitin onto PCNA. Instead, PCNA is heavily sumoylated and SUMO-dependent pathways – including those targeting PCNA – promote viability under these conditions. At last, we demonstrate that transient overexpression of FEN1 in human cell culture leads to an elevation of markers for genome instability. We conclude that overexpression of flap endonuclease is a potent driver of genome instability and mutation, both enabling characteristics of cancer and that this widespread phenomenon has the potential to be an active contributor to cancer formation and evolution.

MATERIALS AND METHODS

Yeast strains and culture conditions

All yeast strains were derived from E133 wild-type cells (Supplementary Table S1) (33). Cultures carrying plasmid-borne galactose inducible constructs were grown in synthetic medium lacking uracil and containing 2% raffinose as a sugar source. Induction of gene expression was accomplished by adding galactose to a final concentration of 2% once cultures had reached an OD_{600} of ∼0.600. All genetic knockouts were generated by polymerase chain reaction (PCR)-mediated gene disruption (34). The *mms21-CH* allele was introduced via a two-fragment PCR method that has been described previously (35). Briefly, one fragment containing *mms21-CH* was generated from genomic DNA using a 5′ primer upstream of the *mms21-CH* locus and a downstream 3′ primer with a region complementary to the 5′ end of a second PCR fragment containing a *LEU2* marker. Equal molar ratios of the two fragments were mixed, denatured at 95°C for 5 min and allowed to anneal at room temperature for 30 min before being transformed into competent yeast cells.

Plasmids

Overexpression of *RAD27*, *rad27-n* and *rad27-FFAA* was under control of an inducible *GAL1-10* promoter in a YEp195SPGAL plasmid backbone (36). These constructs were obtained from D. Gordenin and have been described (5). His_6-PCNA strains were constructed using Yip128-P30-POL30 (a gift from H.D. Ulrich, IMB Mainz). This construct was linearized with AflII and integrated at the genomic *LEU2* locus. Expression was analyzed by western blot to ensure similar protein levels to endogenous untagged PCNA. Endogenous *POL30* was then knocked out via PCR-mediated gene disruption.

Strains with a PCNA-K164R mutation were generated by transformation of a single PCR fragment amplified from pCH1654 (a gift from L. Prakash, UTMB) or derivatives with additional lysine mutations introduced using the QuikChange Lightning Site-Directed Mutagenesis kit (Agilent). The resulting fragment was composed of the PCNA coding sequence and a *LEU2* marker flanked by homology arms targeting it for integration at the endogenous PCNA locus. Integration and incorporation of the mutant allele were confirmed by PCR and sequencing.

The 3xFLAG-FEN1 was transiently overexpressed in 293T cells from a pShuttle-3xFLAG-FEN1 vector under the control of a cytomegalovirus (CMV) promoter (S. Stewart, Washington U).

His_6-PCNA purification

Purification of His_6-PCNA was performed as previously described (12,37). Briefly, cultures were grown to OD_{600}

~0.600 in medium containing 2% raffinose. Galactose was then added to a final concentration of 2% to induce *RAD27* overexpression. In experiments with UV treatment, induction was carried out for 2 h before treatment with 100 J/m^2 of 254 nm light using a UV cross-linker (CL-1000, UVP). After collection, cell pellets were stored at −80°C overnight before processing. The pellets were then subjected to lysis under denaturing conditions and protein extracts were prepared in 8 M urea buffer. His_6-PCNA was bound to Ni-NTA conjugated agarose overnight at room temperature before washing with buffers of decreasing pH to successively increase stringency. Bound His_6-PCNA was eluted with ethylenediaminetetraacetic acid (EDTA)-containing buffer and the eluates were fractionated by sodium dodecyl sulphate-polyacrylamide gel electrophoresis (SDS-PAGE) for western blot analysis with antibodies raised against PCNA, ubiquitin and SUMO.

Protein extraction and western blotting

Protein extracts were isolated by lysing cells under denaturing conditions, precipitating protein with trichloracetic acid, and resuspending the precipitated protein pellet in SDS loading buffer (38). Extracts were fractionated by SDS-PAGE, transferred to a polyvinylidene difluoride (PVDF) membrane and analyzed by western blot with the following antibodies as indicated in each figure; anti-FEN1 (ab2619, Abcam) at a 1:1000 dilution in 5% blocking solution overnight, anti-Rad53 (a gift from JFX Diffley, LRI) at a 1:1000 dilution in 5% blocking solution for 1 h. This antibody was tested in *rad53* mutants (39). Anti-phospho-S129 H2A (ab15083, Abcam) was used at a 1:500 dilution in blocking solution overnight, anti-tubulin (MMS-407R, Covance) at a 1:5000 dilution in 5% blocking solution overnight, anti-PCNA (a gift from B. Stillman, CSHL) at a 1:4000 dilution in TBST for 2 h, anti-ubiquitin (P4D1, Covance) at a 1:1000 dilution in 5% blocking solution overnight, anti-SUMO (a gift from X. Zhao, MSKCC) at a 1:3000 dilution in TBST for 1 h, anti-phospho-S4/8 RPA32 (A300-245A, Bethyl Laboratories) at a 1:2000 dilution in 5% blocking solution overnight, and anti-γH2AX (A300-081A, Bethyl Laboratories) at a 1:2000 dilution in 5% blocking solution overnight. The anti-FEN1 antibody was raised against human FEN1 and only cross-reacted with yeast Rad27 sufficiently to visualize by western blot when Rad27 was overexpressed.

Mutation rate estimation

Mutation rates were estimated using the forward rate of mutations at the *CAN1* locus that conferred resistance to canavanine. Individual colonies were inoculated in medium lacking uracil and containing 2% raffinose as well as 2% galactose. Under these conditions the cultures required 8 days of growth at 25°C to reach saturation. Saturated cultures were washed and appropriate dilutions were plated on medium lacking arginine and containing canavanine (60 mg/l) or on rich medium to obtain a viable cell count. Mutation rates were calculated using Drake's formula and significance was determined using a two-sided Mann–Whitney U-test (40–42). Determinations were made from at least 16 independent cultures for each strain.

Cell cycle analysis

DNA content in yeast cells was measured by flow cytometry using a BD Accuri C6 flow cytometer and Sytox Green (Invitrogen) DNA dye. Measurement of DNA content in 293T cells was carried out using the same machine with propidium iodide (Sigma-Aldrich) as the DNA stain.

Viability analysis

The relative viability of yeast strains was examined in a 'spotting' assay. We began by inoculating 10 ml cultures in medium lacking uracil and containing 2% glucose as a sugar source. These cultures were grown to saturation for 4 days at 25°C, harvested, washed with 10 ml water and resuspended in 5 ml water. The cells in the resulting suspension were quantified and 10-fold serial dilutions were then prepared in a 96-well plate from a starting cell count of 2×10^7. The spots were then plated using a multi-pronged plating instrument on medium lacking uracil and containing either 2% glucose or 2% galactose. Images were taken after 4 days growth at 25°C. Strains containing the *mms21-CH* allele had an inherent growth defect made direct comparison with other strains difficult to visualize. To account for this, 5-fold more cells (10^8) were used as the starting cell count for all *mms21-CH* strains.

Molecular combing

DGY174 (Empty vector), DGY173 (*GAL1pr-RAD27*) and DGY175 (*GAL1pr-rad27FFAA*) were grown at 25°C in medium lacking uracil to mid-logarithmic phase and treated with 150 ng/ml α-factor for 2 h to induce G1 cell-cycle arrest. The 2% w/v galactose was added to induce expression of *GAL1/10* promoter regulated genes, with an additional aliquot of 150 ng/ml α-factor to maintain G1 arrest for an additional 2 h after the addition of galactose. Cells were harvested by centrifugation, washed in ddH_2O and re-suspended in fresh SRG-Ura containing 400 μg/ml BrdU. A total of 100 μg/ml pronase was added to release cells from the α-factor block and cells were harvested after 40 min. Plug preparation, DNA extraction and immunofluorescence were carried out as previously described (43). For each sample at least 50 images of well-dispersed DNA fibers were taken at 63× magnification using an AxioImager.ZI epifluorescence microscope and Axiovision software (Zeiss). Image and data analysis were carried out as previously described (43). The distributions of track lengths and inter-origin distances from two independent experiments were combined.

Human cell culture

The 293T cells were cultured in Dulbecco's modified eagle medium. Transient transfection was carried out with Lipofectamine LTX (Thermo Fisher). In these experiments 25 μg of circular plasmid DNA was transfected into 293T cells at ~60% confluency on a 10 cm plate. Cells were harvested at 24 and 48 h for protein extraction and DNA content analysis by flow cytometry. For preparation of whole cell extracts, cells were lysed in NETN (20 mM Tris–HCl at pH 8.0, 100 mM NaCl, 1 mM EDTA, 0.5% Nonidet P-40 and

protease inhibitors) for 10 min and then centrifuged at 16 000 *g* for 10 min. Cleared lysates were collected, mixed with SDS loading buffer and boiled before fractionation by SDS-PAGE and analysis by western blot with the indicated antibodies. Chromatin fractions were isolated as previously described (44). Briefly, extracts were prepared by lysis in Buffer A (10 mM HEPES pH 7.9, 10 mM KCl, 1.5 mM $MgCl_2$, 0.34 M sucrose, 10% glycerol, 0.1% triton X-100 and protease inhibitors). Insoluble nuclear proteins were isolated by centrifugation and chromatin bound proteins were subsequently released by sonication. Remaining insoluble factors were cleared by centrifugation before fractionation by SDS-PAGE and western blot analysis using the indicated antibodies.

RNA expression analysis

Level 3 RNASeq V2 FPKM files for lung adenocarcinoma patients were downloaded from The Cancer Genome Atlas (TCGA) (https://portal.gdc.cancer.gov). We extracted FEN1 FPKM counts from patient files with matching tumor and normal samples using a custom perl script.

Drug sensitivity analysis of lung cancer cell lines

FEN1 expression levels were obtained from the Cancer Cell Line Encyclopedia (https://portals.broadinstitute.org/ccle) from RNA seq experiments and sorted based on small cell or non-small cell lung cancers from their TCGA classification. Expression levels were then correlated with drug resistance and sensitivity data by cell line from the Genomics of Drug Sensitivity in Cancer database (http://www.cancerrxgene.org/). FEN1 expression levels were sorted into low and high expressing according to their variation from the median $\log_2$ value, 5.96 for non-small cell lung cancer and 6.56 for small cell lung cancer (SCLC). For each compound and cell type, the lowest and highest 30% of FEN1 expressers were plotted and differences in the mean of the two populations were analyzed by a Student's *t*-test with a Welch's correction. The *z*-score denotes the number of standard deviations from zero, which reflects the untreated control. FEN1 expression values and *z*-scores for selected cell lines are listed in Supplementary Table S2.

RESULTS

RAD27 overexpression promotes genome instability

Overexpression of the Rad27 homolog FEN1 has been observed in a variety of different cancers originating from varying tissue types (13–21). We hypothesized that FEN1 overexpression may impact a fundamental enabling characteristic of cancer, such as genome instability. Although this upregulation may simply reflect an increased demand for FEN1 in rapidly dividing cells, we reasoned that the overabundance of a PCNA-binding enzyme with DNA processing activity could also promote genome instability by disrupting normal replication kinetics.

To investigate this possibility, we utilized a galactose inducible overexpression system in *S. cerevisiae*, which allowed us to rapidly overexpress *RAD27* and track the effect on cell-cycle progression and genome maintenance. Asynchronous cultures with a plasmid-borne, galactose inducible copy of *RAD27* (gal-*RAD27*) or an empty control vector (gal-EV) were grown to log phase before addition of galactose. Upon galactose addition, we observed increased accumulation of cells in G1 in all cultures (Figure 1A and B). Importantly, only upon *RAD27* overexpression did we detect a significant accumulation of cells in S phase, indicating difficulty in completing DNA replication (Figure 1A and B). Overexpression of *RAD27* was rapidly observable and coincided with increased phosphorylation of histone H2A at serine (S) 129, a mitosis entry checkpoint 1 (Mec1) target and marker for ssDNA gaps and/or double-strand breaks (DSBs) (Figure 1C) (45–47). We also observed increased phosphorylation of the checkpoint kinase Rad53, further indicating replication stress or DNA damage (Figure 1C) (48). Whereas a baseline level of a high molecular weight form of Rad53 was present in both gal-EV and gal-*RAD27* containing cultures, we noted that only *RAD27* overexpressing cells exhibited a progressive shift of the fast migrating unphosphorylated form to a slower migrating phosphorylated form (marked by arrow heads in Figure 1C). The persistent high-molecular weight form (marked by an asterisk in Figure 1C) likely resulted from culturing cells in the sub-optimal carbon sources raffinose and galactose. There is evidence that culture in sub-optimal carbon sources leads to metabolic stress and a slower transition from G1 into S phase (49). It is therefore possible that the high-molecular weight form of Rad53 represents a modification due to metabolic stress. Taken together, these observations suggested that *RAD27*/*FEN1* overexpression interferes with normal replication progression and causes checkpoint activation.

In agreement with the presence of DNA damage markers, we also observed reduced viability upon deletion of the homologous recombination (HR) gene *RAD52* (Figure 1D). In contrast, there was no such requirement for the non-homologous end joining (NHEJ) factor DNA ligase 4 (Dnl4). If anything, growth was moderately more robust in *dnl4Δ* mutants (Figure 1D). The requirement for *RAD52* but not *DNL4* to tolerate *RAD27* overexpression suggests that overexpression may lead to replication stress and eventually DSBs that require HR but not NHEJ for efficient repair.

PCNA ubiquitination is impaired in *RAD27* overexpressing cells

The finding that *RAD27* overexpressing cells accumulated in S phase with phosphorylated histone H2A-S129 and Rad53 prompted us to further investigate the relationship between flap endonuclease overexpression and replication stress. We examined ubiquitination of PCNA as a marker of replication stress that indicates the presence of ssDNA gaps (24). We purified His_6-tagged PCNA (His_6-PCNA) from *RAD27* overexpressing cells and analyzed its ubiquitination and sumoylation status by western blot (Figure 2A). Treatment with UV light, which is known to induce PCNA ubiquitination was included as a positive control (24). Unexpectedly, *RAD27* overexpression did not trigger PCNA ubiquitination, and it drastically reduced the level of ubiquitination in response to UV light (Figure 2A). In contrast, PCNA

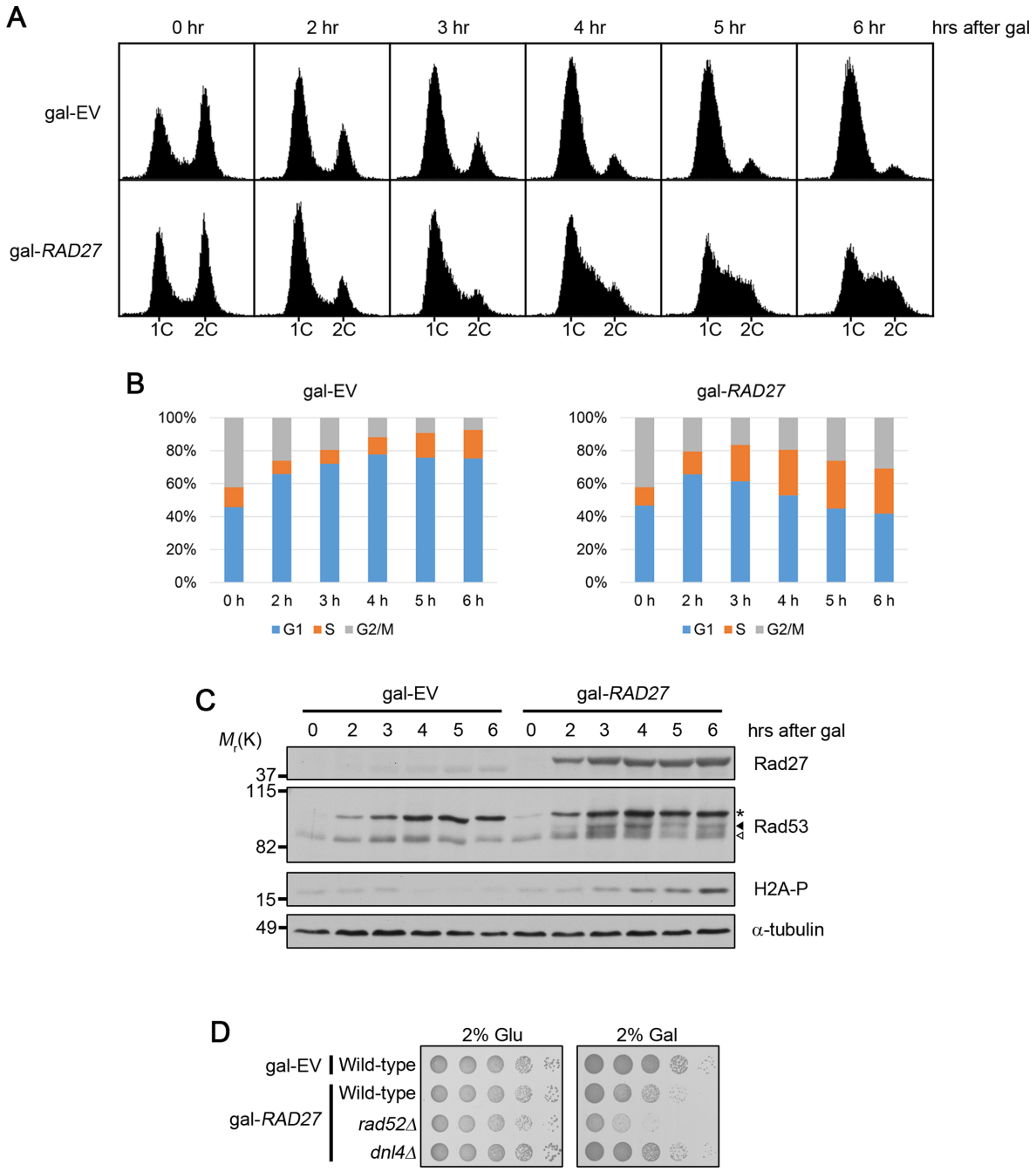

Figure 1. *RAD27* overexpression causes genome instability and impairs S phase progression. (**A**) Strains containing either gal-EV or gal-*RAD27* expression vectors were grown to OD_{600} ~0.600 in synthetic medium lacking uracil and containing 2% raffinose as a sugar source. Galactose was then added to a final concentration of 2% and samples were collected at the indicated time points for analysis by western blot and flow cytometry. DNA content was measured by flow cytometry on a BD Accuri C6 flow cytometer. (**B**) Quantification of the cell-cycle distribution of the profiles in panel B. Quantification was carried out using the BD Accuri C6 software. This result is representative of three independent experiments. (**C**) Samples from the same cultures described above were harvested at the indicated time points and protein extracts were prepared by TCA precipitation. Extracts were fractionated by SDS-PAGE for western blot analysis with anti-Rad27, anti-Rad53, anti-phospho-S129 H2A and anti-tubulin antibodies. The open arrowhead marks unphosphorylated Rad53, the black arrowhead marks phosphorylated Rad53 and the asterisk marks a high-molecular weight form of Rad53 that is induced upon galactose addition. (**D**) The 10-fold serial dilutions of the indicated strains were plated on medium lacking uracil and containing either 2% glucose to suppress gal-*RAD27* or 2% galactose to induce *RAD27* overexpression. Plates were incubated at 25°C for 4 days before imaging.

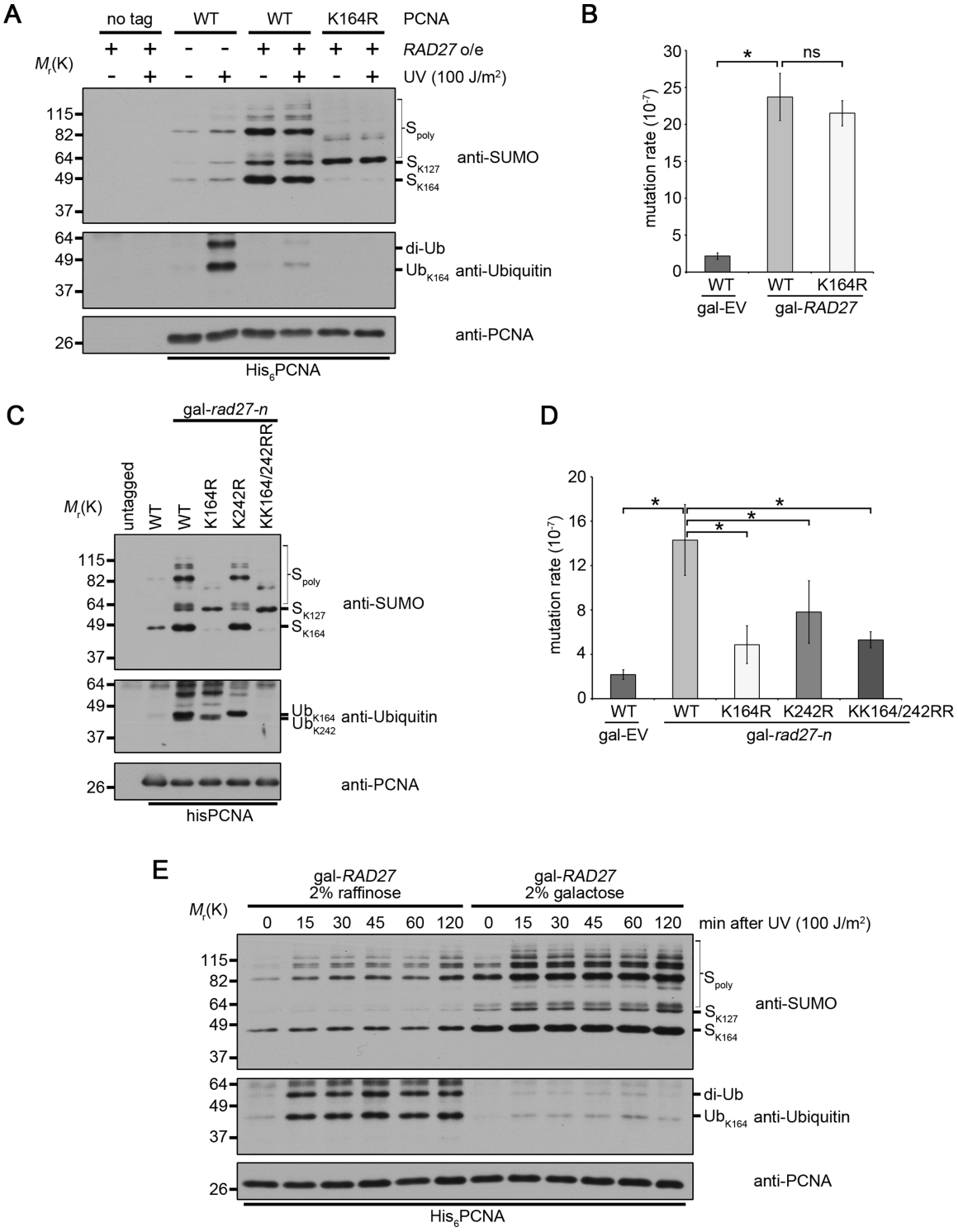

Figure 2. *RAD27* overexpression inhibits PCNA ubiquitination. (**A**) Strains with either untagged PCNA, His_6-PCNA or His_6-PCNA-K164R and all carrying gal-*RAD27* were grown to OD_{600}~0.600 in medium lacking uracil. Overexpression of *RAD27* was then induced by the addition of galactose to a final concentration of 2%. UV treatment was applied 2 h after addition of galactose and the cultures were harvested 1 h later. His_6-PCNA was purified under denaturing conditions and analyzed by western blot with antibodies against PCNA, ubiquitin and SUMO. (**B**) The mutation rate at the *CAN1* locus was measured in the indicated strains after growth to saturation in galactose containing medium. Each bar represents the median of at least 16 independent determinations. Significance was determined using a two-sided Mann–Whitney U-test. (**C**) The indicated strains were grown to OD_{600}~0.600 in complete medium with 2% raffinose before addition of galactose to a final concentration of 2%. Cells were harvested after 3 h and His_6-PCNA was purified under denaturing conditions before analysis by western blot with antibodies against PCNA, ubiquitin and SUMO. (**D**) The mutation rate at the *CAN1* locus was measured as in (B). (**E**) A strain with His_6-PCNA and carrying gal-*RAD27* was grown to OD_{600}~0.600 in medium lacking uracil and containing 2% raffinose. The culture was then split in half with one half receiving an additional 2% raffinose and the other having galactose added to a final concentration of 2%. Both cultures were treated with 100 J/m^2 UV after 2 h. Samples were analyzed as in (A).

sumoylation was strongly enhanced when *RAD27* was overexpressed (Figure 2A). This was likely due to the increase of cells in S phase during which PCNA is sumoylated to recruit Srs2 and inhibit illegitimate recombination between sister chromatids (27,28). We also measured a higher mutation rate at the *CAN1* locus in *RAD27* overexpressing compared to wild-type cells (Figure 2B). As expected, this was independent of PCNA-K164, consistent with the observation that PCNA was not ubiquitinated (Figure 2A). Thus, mutagenesis was operating outside of ubiquitination-dependent translesion synthesis (TLS) (Figure 2B).

We considered the possibility that overexpression of *RAD27 per se* may decrease ubiquitination by occluding PCNA binding surfaces and sterically hindering access for the Rad6–Rad18 ubiquitination complex. To evaluate this hypothesis, we overexpressed another form of Rad27 encoded by the nuclease-dead allele *rad27-n* (D179A). Rad27-n is a dominant negative mutant, which retains the ability to bind PCNA, but is catalytically dead and causes acute growth arrest (5). Overexpression of mutant Rad27 led to robust ubiquitination in the absence of UV, arguing against a model of steric hindrance (Figure 2C). In addition, we also observed increased phosphorylation of H2A-S129 upon *rad27-n* induction (Supplementary Figure S2). This result suggested that the occurrence of DNA damage markers following *RAD27* overexpression was not dependent on the nuclease activity of the enzyme.

Interestingly, in *rad27-n* overexpressing cells we observed ubiquitination of PCNA not only at K164 but at an alternate site, which we mapped to K242 by systematically mutating individual lysines to arginine (Figure 2C). Although K242 was dispensable for normal growth (Supplementary Figure S1), the mutation rate in *rad27-n* expressing cells was significantly increased in a manner that was dependent on both K164 and K242 (Figure 2D). These findings support that TLS was primarily responsible for the increase in the mutation rate under these conditions.

To understand whether ubiquitination of PCNA may have simply been delayed in *RAD27* overexpressing cells due to slowed S phase progression, we analyzed PCNA over the course of 120 min after UV exposure and found that the level of ubiquitination was only minimally enhanced (Figure 2E). From these observations, we concluded that high abundance of catalytically active flap endonuclease interferes with the ubiquitination of PCNA, but that this phenomenon is not due to steric hindrance.

At last, we hypothesized that the drastic increase in sumoylation of PCNA-K164 upon overexpression of *RAD27* may have competitively inhibited ubiquitination at the same residue (Figure 2A). However, a *siz1Δ* mutant strain lacking the E3 SUMO ligase that targets PCNA-K164 was similarly impaired in UV-induced K164 ubiquitination when *RAD27* was overexpressed (Supplementary Figure S3), arguing against this scenario.

Sumoylation enhances viability of *RAD27* overexpressing cells

Since overexpression of *RAD27* did not lead to PCNA ubiquitination and in fact suppressed ubiquitination in response to UV treatment, we predicted that there would not be any genetic interaction between overexpressed *RAD27* and a PCNA-K164R mutation. However, the double mutant gal-*RAD27 pol30-K164R* displayed a very mild but reproducible growth defect (Figure 3A). In contrast, the deletion of PRR pathway components *REV3* and *RAD5* had no effect on viability (Figure 3A). To investigate whether the observed genetic interaction between the *pol30-K164R* allele and *RAD27* overexpression was due to the loss of sumoylation at this residue, we induced flap endonuclease in *siz1Δ* mutants deficient for the E3 SUMO ligase which targets PCNA at K164 (27). Interestingly, the loss of *SIZ1* had a more severe effect on viability than the *pol30-K164R* mutation alone, suggesting that sumoylation of K164 and additional targets of Siz1 may be necessary to fully counteract the genotoxic effects of *RAD27* overexpression (Figure 3B). We also observed a significant reduction in viability in strains carrying a catalytically inactive allele of the E3 SUMO ligase *MMS21* (*mms21-CH*) (Figure 3B). Deletion of *siz2Δ* had no impact on viability. Together, these findings indicate that sumoylation by Siz1 and Mms21 enhances growth under conditions of *RAD27* overexpression.

Sumoylation of PCNA at K164 is thought to primarily act to recruit the helicase/anti-recombinase Srs2 which suppresses illegitimate HR between nascent sister chromatids at the replication fork (27,28). Deletion of *SRS2* resulted in a very mild growth defect, similar to that observed in K164R mutants (Figure 3C). Combination of the two alleles revealed an additive effect in reducing viability, indicating that PCNA-K164 and Srs2 have independent functions under these conditions (Figure 3C). This, in turn, is consistent with Srs2 having a pro-recombination role that is independent of its interaction with PCNA and promotes cell viability (31,32). It may be that Srs2 is required at replication forks in *RAD27* overexpressing cells to inhibit illegitimate recombination, but facilitates HR at DSB sites. *pol30-K164R siz1Δ* mutants on the other hand behaved similarly to *siz1Δ* mutants, further supporting the notion that Siz1 dependent sumoylation, including that of PCNA at K164, is promoting the ability of *RAD27* overexpressing cells to proliferate (Figure 3C).

We next sought to determine whether the *pol30*-K164R, *siz1Δ*, *mms21-CH* or *rad52Δ* alleles led to increased DNA damage sensitivity. Consistent with previous reports, *pol30-K164R*, *mms21-CH* and *rad52Δ* mutants all exhibited enhanced sensitivity to DNA damage even in the absence of *RAD27* overexpression (Figure 4A and B) (50–52). Remarkably, when combined with *RAD27* overexpression, the sensitivity to 4-nitoquinoline 1-oxide (4-NQO), the alkylating drug methyl methanesulfonate (MMS) or replication inhibitor hydroxyurea (HU) was dramatically enhanced (Figure 4A–C). *RAD27* overexpression was sufficient to acutely sensitize cells to 4-NQO, MMS and HU at concentrations that had a minimal effect on the control (gal-EV) strain. For example, *rad52Δ* mutants are moderately sensitive to 0.01% MMS. Overexpression of Rad27 enhanced this sensitivity by three orders of magnitude (Figure 4B). Similarly, *siz1Δ* mutants are relatively insensitive to 4-NQO and MMS, but become highly sensitive when Rad27 is overexpressed (Figure 4A and B). These results suggested that elevated levels of Rad27 simulate DNA repair or DNA damage tolerance pathway deficiencies. This is compounded by our observa-

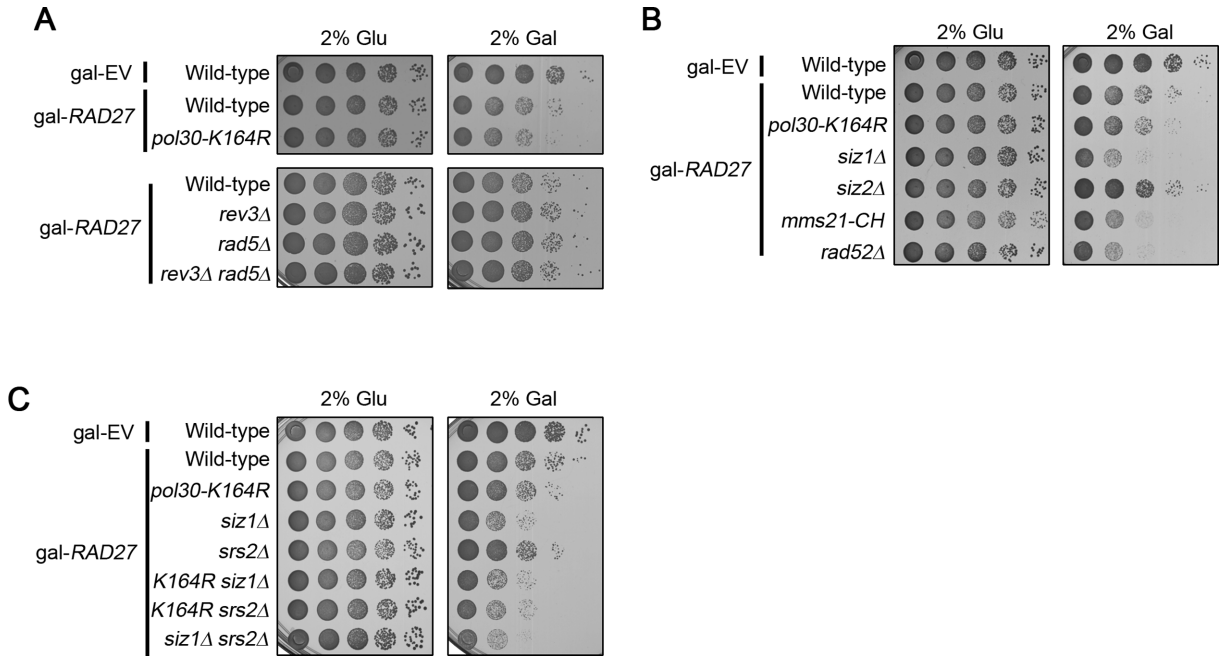

Figure 3. Sumoylation aids in the proliferation of *RAD27* overexpressing cells. (**A**–**C**) 10-fold serial dilutions of the indicated strains were plated on medium lacking uracil and containing either 2% glucose to suppress gal-*RAD27* or 2% galactose to induce *RAD27* overexpression. Plates were incubated at 25°C for 4 days before imaging.

tion that *RAD27* overexpression impeded normal ubiquitination of PCNA and this may provide a mechanistic explanation for the observed sensitivity to DNA damaging agents.

DNA damage in *RAD27* overexpressing cells is dependent on its interaction with PCNA

We demonstrated that overexpression of *RAD27* causes S phase delay, Rad53 checkpoint activation, induction of DNA damage markers and mutation. To better understand whether these effects are dependent on the ability to interact with PCNA, we generated a variant of the overexpression construct carrying a *rad27-FFAA* allele in which two crucial phenylalanine residues (F346, F347) located in the PIP box of Rad27 were mutated to alanines to ablate PCNA binding (5). Remarkably, we found that overexpression of this PCNA binding mutant did not result in any observable increase in phosphorylation of H2A-S129 or Rad53 over that observed in an empty vector control (Figure 5A). Additionally, the severe S-phase delay observed in *RAD27* overexpressing cells was absent when *rad27-FFAA* was overexpressed (Figure 5B and C). We detected a slight increase in G2/M compared to the empty vector controls, which was likely a reflection of the mutant having some problems finishing replication (Figure 5B and C). Furthermore, expression of this mutant in combination with *pol30-K164R*, *siz1Δ*, *mms21-CH* or *rad52Δ*, which all displayed negative genetic interactions with *RAD27* overexpression, did not result in growth inhibition (Figure 5D and E). In fact, the *rad27-FFAA* mutation rescued the proliferation defect and the other observed genome instability phenotypes inherent to *RAD27* overexpression (Figure 5D and E; Supplementary Figure S4). Furthermore, single-molecule analysis of replicating fibers by DNA combing revealed a significantly shorter track length in *RAD27* overexpressing cells compared to the empty vector control (Figure 6A–C and Supplementary Figure S5). *RAD27* overexpressing cells also exhibited a reduction in inter-origin distance, consistent with the notion that dormant origins are activated at an elevated level (Figure 6D). Both effects were ameliorated by the *rad27-FFAA* allele (Figure 6C and D). Together, these results suggested that *RAD27* overexpression interfered with normal progression of active replication forks and that this interference is dependent on the interaction of Rad27 with PCNA.

Overexpression of FEN1 in 293T cells causes DNA damage

Overexpression of flap endonuclease in yeast impaired DNA replication and promoted checkpoint activation as well as a notable increase in markers for DNA damage. To investigate whether the same held true for overexpression of the human Rad27 homolog FEN1, we transiently transfected 293T cells with a vector encoding FLAG-tagged FEN1 under control of a CMV promoter. We selected this cell line because it is known for its capacity to produce significant amounts of protein from transgenes. Transient overexpression of FLAG-FEN1 led to a slight elevation in PCNA ubiquitination and a more significant increase in the phosphorylation of RPA32-S4/S8, an ataxia telangiectasia mutated (ATM) target and marker for DSB processing (Figure 7A) (53,54). Levels of γH2AX, a marker for DSB formation were also increased at the 24 and 48 h time points (55). These findings are indicative of DNA damage induction upon FLAG-FEN1 expression. This was accompanied by increased phosphorylation of the checkpoint kinases Chk1 (S345) and Chk2 (T68), ATR and ATM targets,

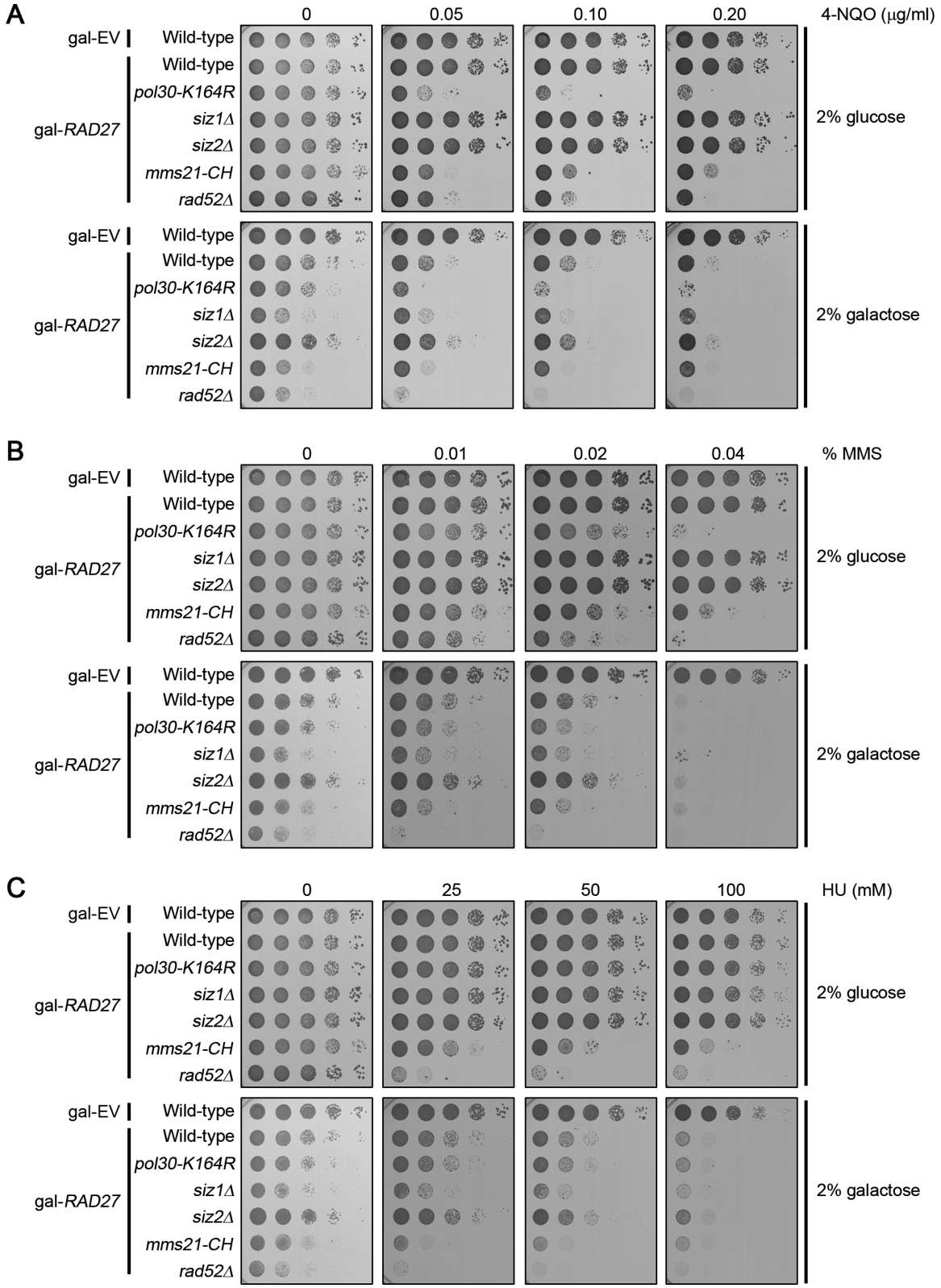

Figure 4. *RAD27* overexpressing cells are acutely sensitive to DNA damage. (**A**) The 10-fold serial dilutions of the indicated strains were plated on medium lacking uracil and containing either 2% glucose to suppress gal-*RAD27* or 2% galactose to induce *RAD27* overexpression. The medium contained 0.05, 0.10 or 0.20 μg/ml 4-NQO as indicated. Plates were incubated at 25°C for 4 days before imaging. (**B**) The 10-fold serial dilutions of the indicated strains were plated on medium lacking uracil and containing either 2% glucose to suppress gene expression or 2% galactose to induce overexpression. The medium contained 0.005, 0.01 or 0.02% MMS as indicated. Plates were incubated at 25°C for 4 days before imaging. (**C**) The 10-fold serial dilutions of the indicated strains were plated on medium lacking uracil and containing either 2% glucose to suppress gene expression or 2% galactose to induce overexpression. The medium contained 25, 50 or 100 mM MMS as indicated. Plates were incubated at 25°C for 4 days before imaging.

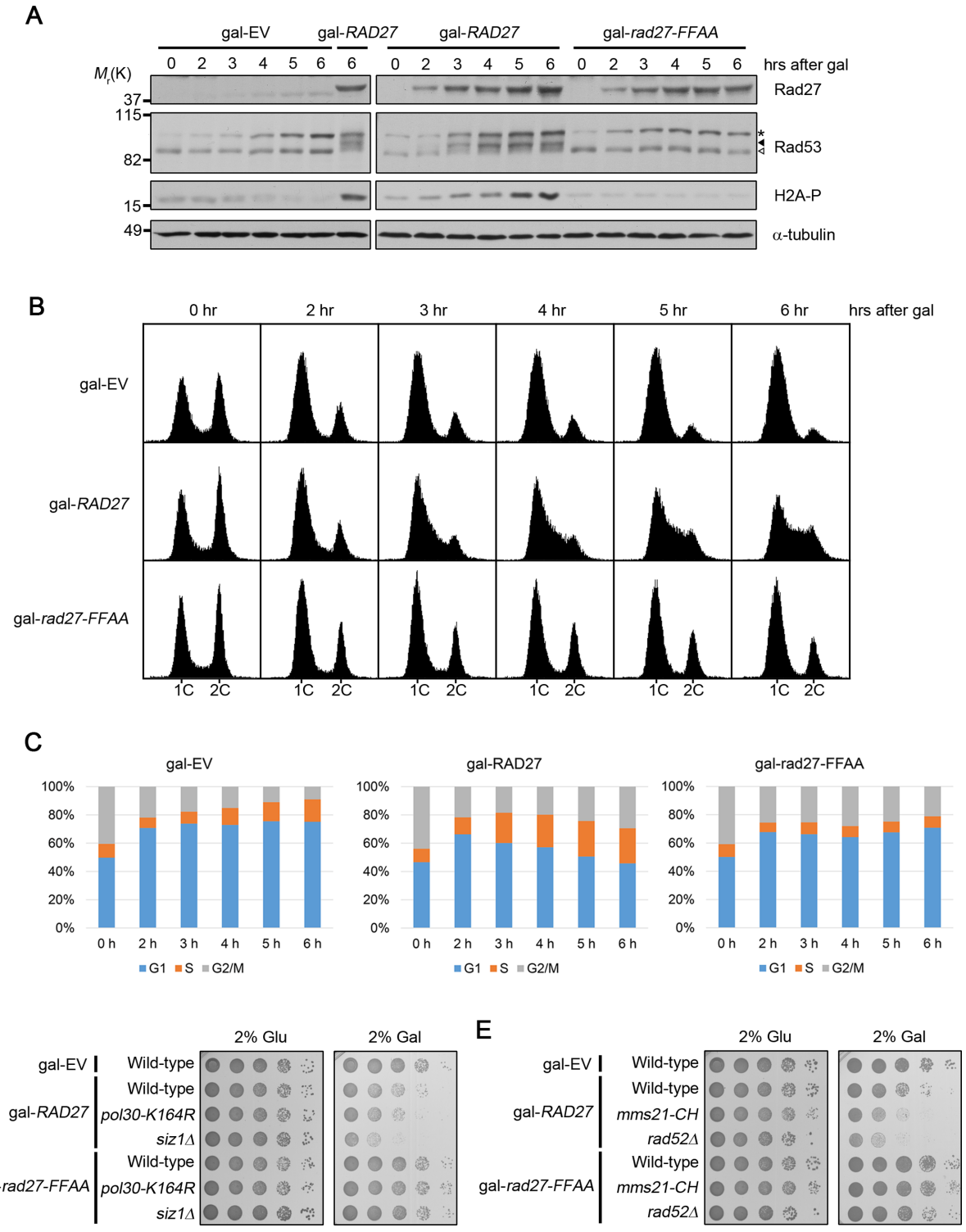

Figure 5. Rad27–PCNA interaction mediates the effects of *RAD27* overexpression. (**A**) Strains containing gal-EV, gal-*RAD27* or gal-*rad27-FFAA* expression vectors were grown to OD_{600} ~0.600 in synthetic medium lacking uracil and containing 2% raffinose as a sugar source. Galactose was then added to a final concentration of 2% and samples were collected at the indicated time points for analysis by western blot and flow cytometry. Protein extracts were prepared by TCA precipitation and fractionated by SDS-PAGE for western blot analysis with anti-Rad27, anti-Rad53, anti-phospho-S129 H2A and anti-tubulin antibodies. The open arrowhead marks unphosphorylated Rad53, the black arrowhead marks phosphorylated Rad53 and the asterisk marks a high-molecular weight form of Rad53 that is induced upon galactose addition. (**B**) Samples from the same cultures described above were harvested at the indicated time points and DNA content was measured by flow cytometry on a BD Accuri C6 flow cytometer. (**C**) Quantification of the cell-cycle distribution of the profiles in panel B. Quantification was carried out using the BD Accuri C6 software. (**D** and **E**) The 10-fold serial dilutions of the indicated strains were plated on medium lacking uracil and containing either 2% glucose to suppress overexpression or 2% galactose to induce *RAD27* or *rad27-FFAA* overexpression. Plates were incubated at 25°C for 4 days before imaging.

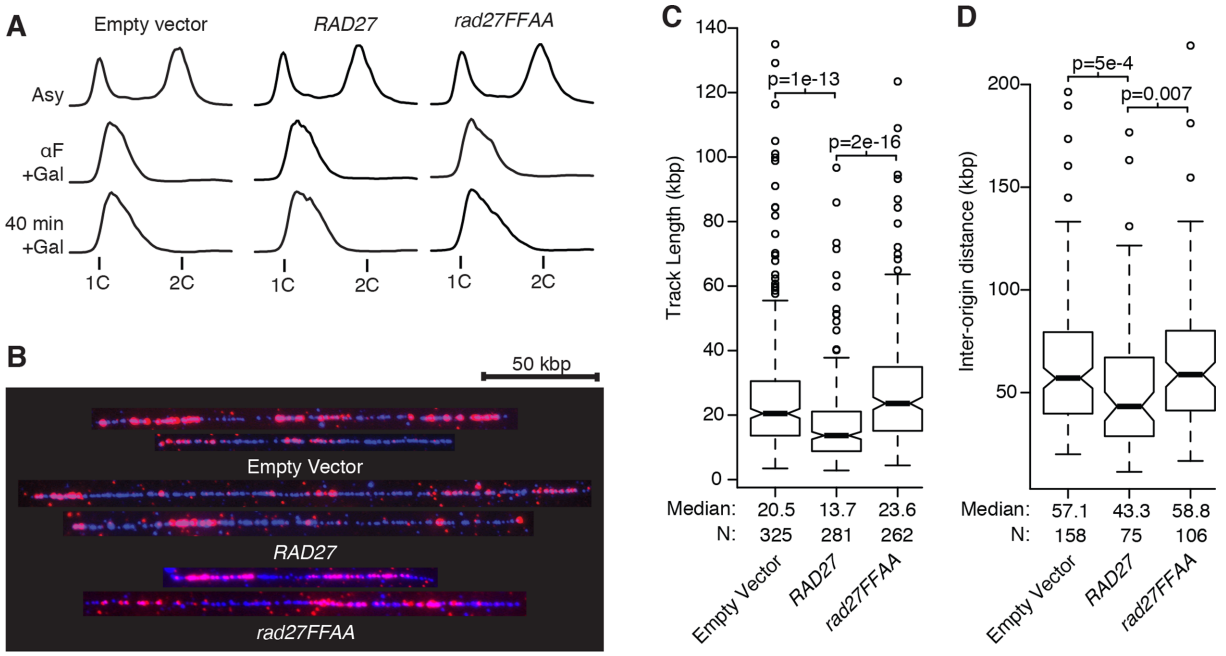

Figure 6. Overexpression of *RAD27* causes defects in replication fork progression. (**A**) Cells carrying *RAD27* or *rad27-FFAA* under the control of the *GAL1/10* promoter, or carrying the empty vector, were arrested in G1 phase and released into S phase in the presence of galactose. DNA contents were measured by flow cytometry of logarithmic phase cells (Asy), G1 arrested cells (αF+Gal) and cells released into S phase for 40 min (40 min+Gal). The 1C and 2C DNA content peaks are indicated. (**B**) Representative chromosome fibers from DNA combing analysis used for BrdU track length and inter-origin distance analysis are shown. Individual fibers were extracted from different micrographs and assembled using Photoshop. The scale bar is 50 kbp. (**C**) Distribution of BrdU track lengths, and (**D**) inter-origin distances, for cells overexpressing *RAD27*, *rad27FFAA* and control cells (empty vector) sampled 40 min after release into S phase are presented as boxplots. The horizontal bars indicate median BrdU tract lengths (in pink) and inter-origin distances, which are also indicated below the graph. The boxes span the first through third quartiles, the whiskers extend to the last data points within 1.5× the interquartile range and outliers are plotted as circles. *P*-values were determined using a two-sided Mann–Whitney U-test.

respectively. In contrast to our findings in yeast, we did not observe any significant alterations in the cell-cycle distribution of these cultures as measured by DNA content (Figure 7B), similar to what has been reported previously (56).

Overexpression of FEN1 has recently been associated with enhanced proliferation and poor prognosis in non-small-cell lung cancers (NSCLC) (57). Another study of FEN1 overexpressing NSCLCs demonstrated that FEN1 inhibition impaired tumor growth and increased therapeutic response in murine xenograft models (58). As a result, we wanted to independently confirm that overexpression of FEN1 was broadly observable in lung adenocarcinomas, a subtype of NSCLC. Relative expression levels of FEN1 mRNA in 18 matched normal and tumor tissues from lung adenocarcinoma patients were obtained from TCGA (https://cancergenome.nih.gov/). In accordance with what has been previously reported, we found overexpression of FEN1 to be prevalent in the vast majority of tumor samples (Figure 7C) (16,57–60). The median level of overexpression was ∼5-fold with individual samples and ranged as high as 10-fold over normal tissue.

Overexpression of FEN1 alters drug sensitivity in small cell lung cancer cell lines

It appears that increased expression of flap endonuclease has a conserved effect between yeast and human cell systems marked by a significant increase in factors that trigger genome instability. Because overexpression of *RAD27* rendered yeast cells hypersensitive to HU and loss of *RAD52*, we asked whether high expression of FEN1 mRNA in lung cancer cell lines affected their sensitivity to drugs known to interfere with the DNA damage response or DNA replication. We analyzed both NSCLC and SCLC cell lines. We compared the lowest to the highest FEN1 expressers (bottom 30% versus top 30%) and determined their sensitivities to the ATM inhibitor CP466722, the replication inhibitor methotrexate and the DNA protein kinase (DNA-PK) inhibitor NU7441 by mining the Genomics of Drug Sensitivity in Cancer database (http://www.cancerrxgene.org/). A positive *z*-score indicates drug resistance, whereas a negative *z*-score indicates drug sensitivity. Although the response among NSCLC cell lines did not show a significant difference between low and high FEN1 expressers, SCLC cells displayed a significant difference in their sensitivity to the ATM inhibitor CP466722 (Figure 8). High FEN1 expression levels correlated with a higher sensitivity to CP466722, but not to the DNA-PK inhibitor NU7441 (Figure 8). Since ATM is required to trigger DSB repair by HR (61), and DNA-PK is necessary for NHEJ (62), these results argue that the overexpression of FEN1 in SCLC cells is associated with an increased dependence on HR, but not NHEJ, similar to our results in *RAD27* overexpressing yeast cells (Figure 1D). SCLC cells that express high levels of FEN1 also seemed to be more sensitive to methotrexate, an inhibitor of dihydrofolate reductase that is required for thymidylate synthesis (63), although the *P*-value for this comparison was

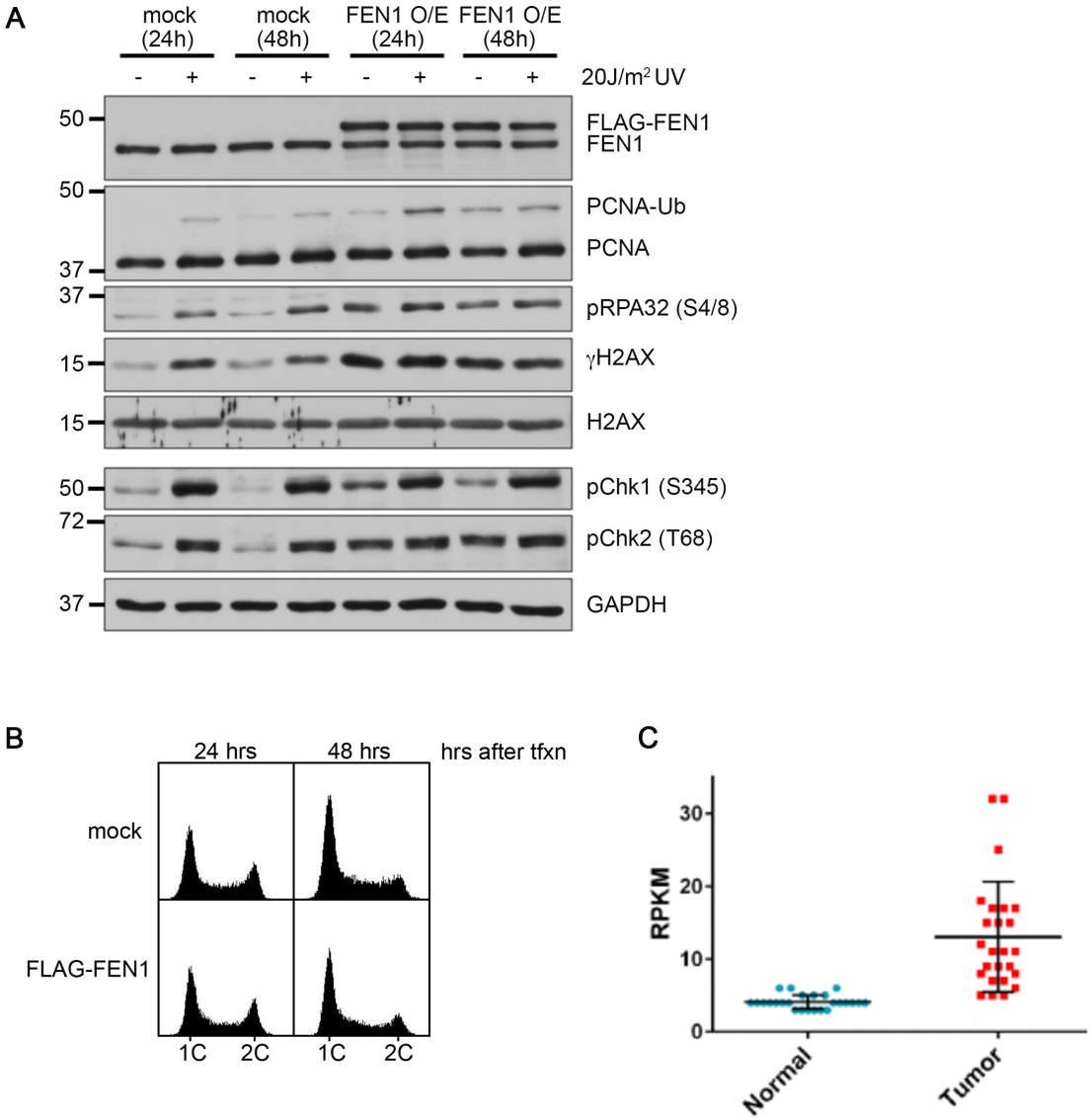

Figure 7. FEN1 overexpression promotes genome instability. (**A**) 293T cells were either mock transfected or transiently transfected with FLAG-FEN1 under control of a CMV promoter and collected 24 or 48 h after transfection. Treatment with 10 J/m^2 UV was included as a positive control for DNA damage. UV-treated cultures were harvested 24 h after irradiation. Whole cell extracts were isolated and fractionated by SDS-PAGE for western blot analysis with anti-phospho-S4/8 RPA32, anti-PCNA, anti-phospho-S345 Chk1, anti-phospho-T68 Chk2, anti-γH2AX, anti-H2AX, anti-FEN1 and anti-GAPDH. (**B**) A portion of the cells collected from the experiment described in (A) were fixed in ethanol and DNA content was measured by flow cytometry on a BD Accuri C6 flow cytometer. (**C**) FEN1 reads per kilobase of transcript per million mapped reads (RPKM) from lung adenocarcinoma and matched normal tissue were compared. Of the 162 RNA seq datasets available, these 50 were paired tumor/normal samples from 25 patients. Lines indicate mean values and bars represent standard deviations. Source: TCGA: http://cancergenome.nih.gov/.

slightly above 0.05 (Figure 8). These findings suggest that overexpression of FEN1 can be linked to altered drug sensitivities in specific cancers, but that the impact is cell type dependent.

DISCUSSION

Here, we have demonstrated that overexpression of the FEN1 homolog Rad27 in yeast impairs DNA replication in a manner that is dependent on its interaction with PCNA. We interpret the presence of DNA damage markers, the activation of Rad53 as well as the accumulation of TLS-independent mutations as clear indicators of genome instability. This is consistent with a previous report by Aguilera and colleagues, however, the authors did not attempt to uncover the underlying mechanisms (64), which was the focus of our study. Overexpression of FEN1 has been observed in cancers derived from a variety of tissue types at levels approaching 50-fold greater than matched normal tissues in some cases (16). With this in mind, we modeled FEN1 overexpression using the strong *GAL1/10* promoter to enforce overexpression of its counterpart in yeast. This promoter has the dual advantage of inducible control and driving expression at sufficiently high levels to recapitulate what has been observed in human cancers.

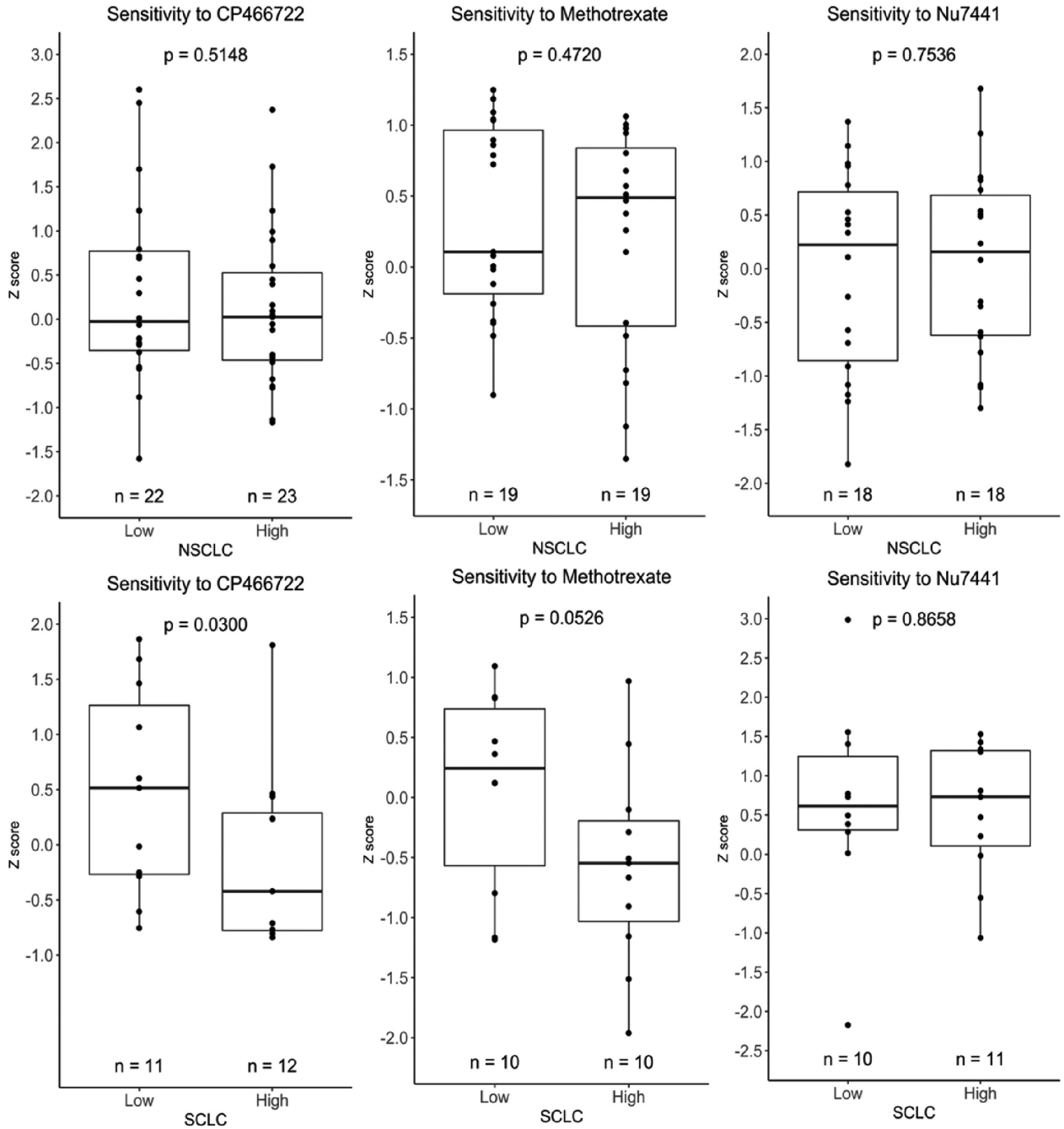

Figure 8. Sensitivity to CP466722, methotrexate and NU7441 in selected NSCLC and SCLC cell lines that either display low or high mRNA expression of FEN1. The Cancer Cell Line Encyclopedia (https://portals.broadinstitute.org/ccle) was analyzed for FEN1 mRNA expression of NSCLC (top) and SCLC (bottom) cell lines according to TCGA classification. Low expression constitutes the bottom 30%, whereas high expression constitutes the top 30% of all identified cell lines in each group. Sensitivity to CP466722, methotrexate and NU7441 was extracted from the Genomics of Drug Sensitivity in Cancer database (http://www.cancerrxgene.org/). For each compound and cell type, the lowest and highest FEN1 expressers were plotted and differences in the mean of the two populations were analyzed by a Student's *t*-test with a Welch's correction. *P*-values are indicated on top of each panel. *z*-scores represent increasing drug resistance (above zero) or sensitivity (below zero).

Sumoylation suppresses the effects of *RAD27* overexpression

Work over the past two decades has vastly increased our understanding of the complex networks of posttranslational modifications in response to replication stress and DNA damage (52,65). Among these, the ubiquitination of PCNA at the conserved residue K164 plays a crucial role in coordinating PRR pathways (23). Because the appearance of this modification is a sensitive marker for replication stress, we were surprised that *RAD27* overexpression not only failed to elicit this response, but suppressed it following UV treatment. This may, at least partly, be explained by the finding that replication fork progression is impaired when cells overexpress wild-type Rad27. Since the detection of UV lesions in S phase is dependent on their active encounter with a replication fork, it is possible that reduced fork progression significantly decreased the probability of such encounters. Although net nucleotide incorporation was only ∼2-fold diminished in *RAD27* overexpressing cells under otherwise unperturbed conditions, we do not know whether origin activation and/or fork progression might have been altered in these cells following UV radiation. It is conceivable that other, as-of-yet unidentified mechanisms were responsible for the observed lack of PCNA ubiquitination.

The observation that sumoylation, but not ubiquitination of PCNA at K164 enhanced the viability of *RAD27* overexpressing cells prompted us to investigate the role of the three yeast SUMO ligases under these conditions. Genetic interaction studies with mutant alleles of *SIZ1*, *SIZ2* and *MMS21* revealed a significant decrease in viability in combination with *siz1Δ* and *mms21-CH*, but not *siz2Δ*, suggestive of broader applications for sumoylation beyond the attachment to PCNA. Although our analysis of *RAD27* overexpressing cells identified PCNA as an abundant SUMO target, it is possible that additional Siz1 and Mms21 targets of importance remain unidentified. More sensitive and quantitative techniques will be necessary to identify these targets. It is also possible that multiple targets of low individual importance have an additive effect on viability. Additional studies will be necessary to fully understand the role of SUMO in mediating Rad27-induced replication stress.

Interaction with PCNA mediates *RAD27* overexpression effects

Our finding that mutation of the *RAD27* PIP box in *rad27-FFAA* mutants abrogates the negative impacts of *RAD27* overexpression suggests two possible mechanisms by which expression of the wild-type enzyme imperils genome stability. First, overabundance of Rad27 as a PCNA interacting protein might 'passively' disrupt the kinetics of replication by impeding the ability of other PCNA binding replication factors to be appropriately localized. Such a model has been proposed to explain the detrimental effects of DNA ligase I overexpression on genome stability and is also thought to be one of the mechanisms by which p21 regulates DNA replication (66,67).

In addition, the catalytic activity of Rad27 might antagonize Okazaki fragment maturation in an 'active' manner by enhanced resection of nascent DNA on the lagging strand. Unfortunately, we were not able to directly test this model as a catalytically dead mutant of *RAD27* (*rad27-n*) displays a dominant negative phenotype (5). Interestingly, upon Rad27-n overexpression, we observed ubiquitination of PCNA at the previously unreported site of K242. It is notable that this modification appeared to promote TLS. The dominant negative phenotype of Rad27-n is thought to be the result of sustained substrate binding by the catalytically dead enzyme, which is unable to complete its catalytic cycle and will not release (5). The enzyme substrate complex therefore acts as an impediment to processing by alternative enzymes, severely disrupting Okazaki fragment processing and delaying the completion of DNA replication. As shown previously, a mutation in the PIP box of Rad27-n alleviates the dominant negative phenotype of the mutant (5). This demonstrates that the PIP box mutation not only abrogates the Rad27:PCNA physical interaction, but it also must impair substrate binding and processing *in vivo* (68).

The fact that all observed growth and genome instability phenotypes upon *RAD27* overexpression are completely dependent on the interaction between Rad27 and PCNA and result in a severe S phase delay argues that the effect is directly linked to the process of DNA replication. We can speculate that due to the well described role of Rad27 in Okazaki fragment processing, disruption of this process is a likely side-effect of overexpression. It is possible that too much flap endonuclease present during Okazaki fragment processing interferes with RNA primer removal, fill-in DNA synthesis and eventual ligation, leading to unligated nicks (1,2,69). If left unrepaired, these nicks would form DSBs during the next round of replication, explaining the observed dependence on HR of *RAD27* overexpressing cells. This is consistent with a recent study by Aguilera and colleagues that demonstrated an increase in recombination frequency and Rad52 foci formation when *RAD27* is overexpressed (64). However, where we observed severe growth inhibition in *rad52Δ* mutants when overexpressing *RAD27,* Aguilera and colleagues reported no such growth defect. It is possible that this discrepancy results from a strain-specific effect, but the origin of any such effect is unclear. We have further expanded on this study by identifying that the DNA damage sensitivity observed by both laboratories is likely due to a suppression of PRR resulting from inhibited PCNA-K164 ubiquitination. We have also identified that the genotoxic effects of Rad27 overexpression are dependent on its ability to physically interact with PCNA, firmly linking these effects to replication dysfunction.

RAD27 overexpression causes DNA damage sensitivity

One of the more striking phenotypes that we observed upon Rad27 overexpression was an acute sensitivity to DNA damage. High abundance of flap endonuclease rendered multiple strains uniformly sensitive to both 4-NQO and MMS treatment at concentrations that failed to impact the growth of control cells that harbored an empty vector. Considering that Rad27 is involved in long patch BER, which is the primary pathway for removal of MMS-induced lesions, it is somewhat counterintuitive that overexpression would sensitize cells to this type of damage (8,70). Nevertheless, we propose two reasons that may explain why this is the case. First, our data suggests that *RAD27* overexpression leads to genome instability and impaired DNA replication.

If these cells are already experiencing considerable difficulty with replication they may be unable to tolerate additional damage and easily succumb to drug treatment. Second, we observed that ubiquitination of PCNA in response to DNA damage was severely reduced. It has been well established that both 4-NQO and MMS treatment lead to an increased dependence on PRR for viability (23,50). It is therefore possible that the inability to ubiquitinate PCNA and activate PRR renders these cells highly sensitive to DNA damaging agents. If this relationship between flap endonuclease overexpression and genotoxic sensitivity is conserved in human cancer cells, it may offer an effective therapeutic target for cancers with high levels of FEN1. Because the mode of action for many clinical chemotherapeutics relies on causing damage to DNA or otherwise inducing replication stress, this would be a highly implementable strategy with a readily identifiable marker in FEN1. Indeed, we show here that SCLC cell lines that highly overexpress FEN1 are significantly more sensitive to the ATM inhibitor CP466722 than those with low FEN1 expression. Importantly, our data also demonstrates that differences in drug response are not always associated with FEN1 expression levels, but may vary from cell type to cell type.

FEN1 overexpression and cancer

Overexpression of FEN1 in cancers from multiple tissues may suggest simply that dividing cancer cells require elevated levels of this replication factor to enable proliferation. However, our finding that overexpression of flap endonuclease in both yeast and human systems is a potent source of genome instability raises the possibility that overabundance of FEN1 presents an active mechanism to drive cancer evolution irrespective of tissue type. Based solely on the results presented in this study, it is impossible to determine whether FEN1 overexpression is a driving factor in carcinogenesis, a promoter of cancer progression or a combination of the two. For example, methylation of FEN1 at K377 by the methyltransferase SET7 during S phase has been implicated in defying replication stress (71). It is currently unknown if all of FEN1 is properly modified when overexpressed, but a lack thereof could directly contribute to an increase in DNA damage. Similarly, the cell cycle-specific turnover of FEN1 by SUMO-dependent ubiquitination-mediated degradation may no longer function properly when the enzyme is highly overexpressed (56). Not surprisingly, inhibition of FEN1 has already been investigated as a potential chemotherapeutic strategy with promising results, although none of these studies have sufficiently analyzed the effect of FEN1 inhibitors specifically in cancers with elevated expression levels (72–74). Such studies will be necessary to determine whether some cancers become 'addicted' to overexpression and whether this is exploitable as a therapeutic strategy.

In summary, we report that overexpression of flap endonuclease impairs DNA replication leading to S phase delay, DNA damage and mutation in a manner that is dependent on its interaction with PCNA. Furthermore, overabundance of Rad27 impairs ubiquitination of PCNA in response to DNA damaging agents and renders these cells acutely sensitive to DNA damage. Our findings provide evidence that this common occurrence in cancer cells may not be simply a passenger effect but must be considered as a driver of genome instability.

SUPPLEMENTARY DATA

Supplementary Data are available at NAR Online.

ACKNOWLEDGEMENTS

The authors wish to acknowledge the Masonic Cancer Center, University of Minnesota Flow Cytometry Shared Resource for technical assistance. Reagents were kindly provided by D. Gordenin, P.M.J. Burgers, B. Stillman, J.F.X. Diffley, X. Zhao, L. Prakash and H.D. Ulrich. We thank Ya-Chu Chang for help with generating figures. At lats, we would like the thank members of the Bielinsky laboratory for helpful insights and discussions.

FUNDING

National Institutes of Health (NIH) [GM074917 to A.K.B.]; Canadian Cancer Society Research Institute, Impact Grant [702310 to G.W.B.]; Masonic Cancer Center at the University of Minnesota, Brainstorm Award (to A.K.B.); The Graduate School at the University of Minnesota Doctoral Dissertation Fellowship (to J.R.B.); Natural Sciences and Engineering Research Council of Canada PGS-D Award (to D.G.). Funding for open access charge: NIH [R01GM074917].
Conflict of interest statement. None declared.

REFERENCES

1. Ayyagari,R., Gomes,X.V., Gordenin,D.A. and Burgers,P.M. (2003) Okazaki fragment maturation in yeast I. Distribution of functions between FEN1 and DNA2. *J. Biol. Chem.*, **278**, 1618–1625.
2. Jin,Y.H., Ayyagari,R., Resnick,M.A., Gordenin,D.A. and Burgers,P.M. (2003) Okazaki fragment maturation in yeast II. Cooperation between the polymerase and 3′–5′-exonuclease activities of Pol δ in the creation of a ligatable nick. *J. Biol. Chem.*, **278**, 1626–1633.
3. Stodola,J.L. and Burgers,P.M. (2016) Resolving individual steps of Okazaki-fragment maturation at millisecond timescale. *Nat. Struct. Mol. Biol.*, **23**, 402–408.
4. Burgers,P.M. (2009) Polymerase dynamics at the eukaryotic DNA replication fork. *J. Biol. Chem.*, **284**, 4041–4045.
5. Gary,R., Park,M.S., Nolan,J.P., Cornelius,H.L., Kozyreva,O.G., Tran,H.T., Lobachev,K.S., Resnick,M.A. and Gordenin,D.A. (1999) A novel role in DNA metabolism for the binding of Fen1/Rad27 to PCNA and implications for genetic risk. *Mol. Cell. Biol.*, **19**, 5373–5382.
6. Chapados,B.R., Hosfield,D.J., Han,S., Qiu,J., Yelent,B., Shen,B. and Tainer,J.A. (2004) Structural basis for FEN-1 substrate specificity and PCNA-mediated activation in DNA replication and repair. *Cell*, **116**, 39–50.
7. Tsutakawa,S.E., Classen,S., Chapados,B.R., Arvai,A.S., Finger,L.D., Guenther,G., Tomlinson,C.G., Thompson,P., Sarker,A.H. and Shen,B. (2011) Human flap endonuclease structures, DNA double-base flipping, and a unified understanding of the FEN1 superfamily. *Cell*, **145**, 198–211.
8. Memisoglu,A. and Samson,L. (2000) Base excision repair in yeast and mammals. *Mutat. Res.*, **451**, 39–51.
9. Reagan,M.S., Pittenger,C., Siede,W. and Friedberg,E.C. (1995) Characterization of a mutant strain of *Saccharomyces cerevisiae* with a deletion of the *RAD27* gene, a structural homolog of the *RAD2* nucleotide excision repair gene. *J. Bacteriol.*, **177**, 364–371.

10. Tishkoff,D.X., Filosi,N., Gaida,G.M. and Kolodner,R.D. (1997) A novel mutation avoidance mechanism dependent on *S. cerevisiae RAD27* is distinct from DNA mismatch repair. *Cell*, **88**, 253–263.
11. Freudenreich,C.H., Kantrow,S.M. and Zakian,V.A. (1998) Expansion and length-dependent fragility of CTG repeats in yeast. *Science*, **279**, 853–856.
12. Becker,J.R., Pons,C., Nguyen,H.D., Costanzo,M., Boone,C., Myers,C.L. and Bielinsky,A.-K. (2015) Genetic interactions implicating postreplicative repair in okazaki fragment processing. *PLoS Genet.*, **11**, e1005659.
13. Kim,J.-M., Sohn,H.-Y., Yoon,S.Y., Oh,J.-H., Yang,J.O., Kim,J.H., Song,K.S., Rho,S.-M., Yoo,H.S. and Kim,Y.S. (2005) Identification of gastric cancer–related genes using a cDNA microarray containing novel expressed sequence tags expressed in gastric cancer cells. *Clin. Cancer Res.*, **11**, 473–482.
14. Lam,J.S., Seligson,D.B., Yu,H., Li,A., Eeva,M., Pantuck,A.J., Zeng,G., Horvath,S. and Belldegrun,A.S. (2006) Flap endonuclease 1 is overexpressed in prostate cancer and is associated with a high Gleason score. *BJU Int.*, **98**, 445–451.
15. Singh,P., Yang,M., Dai,H., Yu,D., Huang,Q., Tan,W., Kernstine,K.H., Lin,D. and Shen,B. (2008) Overexpression and hypomethylation of flap endonuclease 1 gene in breast and other cancers. *Mol. Cancer Res.*, **6**, 1710–1717.
16. Nikolova,T., Christmann,M. and Kaina,B. (2009) FEN1 is overexpressed in testis, lung and brain tumors. *Anticancer Res.*, **29**, 2453–2459.
17. Abdel-Fatah,T.M., Russell,R., Albarakati,N., Maloney,D.J., Dorjsuren,D., Rueda,O.M., Moseley,P., Mohan,V., Sun,H. and Abbotts,R. (2014) Genomic and protein expression analysis reveals flap endonuclease 1 (FEN1) as a key biomarker in breast and ovarian cancer. *Mol. Oncol.*, **8**, 1326–1338.
18. Zhang,B., Jia,W.-H., Matsuda,K., Kweon,S.-S., Matsuo,K., Xiang,Y.-B., Shin,A., Jee,S.H., Kim,D.-H. and Cai,Q. (2014) Large-scale genetic study in East Asians identifies six new loci associated with colorectal cancer risk. *Nat. Genet.*, **46**, 533–542.
19. Hwang,J.-C., Sung,W.-W., Tu,H.-P., Hsieh,K.-C., Yeh,C.-M., Chen,C.-J., Tai,H.-C., Hsu,C.-T., Shieh,G.S. and Chang,J.-G. (2015) The overexpression of FEN1 and RAD54B may act as independent prognostic factors of lung adenocarcinoma. *PLoS One*, **10**, e0139435.
20. He,L., Zhang,Y., Sun,H., Jiang,F., Yang,H., Wu,H., Zhou,T., Hu,S., Kathera,C.S. and Wang,X. (2016) Targeting DNA Flap endonuclease 1 to impede breast cancer progression. *EBioMedicine*, **14**, 32–43.
21. Narayan,S., Jaiswal,A.S., Law,B.K., Kamal,M.A., Sharma,A.K. and Hromas,R.A. (2016) Interaction between APC and Fen1 during breast carcinogenesis. *DNA Repair*, **41**, 54–62.
22. Ulrich,H.D. (2009) Regulating post-translational modifications of the eukaryotic replication clamp PCNA. *DNA Repair*, **8**, 461–469.
23. Hoege,C., Pfander,B., Moldovan,G.-L., Pyrowolakis,G. and Jentsch,S. (2002) *RAD6*-dependent DNA repair is linked to modification of PCNA by ubiquitin and SUMO. *Nature*, **419**, 135–141.
24. Davies,A.A., Huttner,D., Daigaku,Y., Chen,S. and Ulrich,H.D. (2008) Activation of ubiquitin-dependent DNA damage bypass is mediated by replication protein a. *Mol. Cell*, **29**, 625–636.
25. Prakash,S., Johnson,R.E. and Prakash,L. (2005) Eukaryotic translesion synthesis DNA polymerases: specificity of structure and function. *Annu. Rev. Biochem.*, **74**, 317–353.
26. Branzei,D. (2011) Ubiquitin family modifications and template switching. *FEBS Lett.*, **585**, 2810–2817.
27. Pfander,B., Moldovan,G.-L., Sacher,M., Hoege,C. and Jentsch,S. (2005) SUMO-modified PCNA recruits Srs2 to prevent recombination during S phase. *Nature*, **436**, 428–433.
28. Papouli,E., Chen,S., Davies,A.A., Huttner,D., Krejci,L., Sung,P. and Ulrich,H.D. (2005) Crosstalk between SUMO and ubiquitin on PCNA is mediated by recruitment of the helicase Srs2p. *Mol. Cell*, **19**, 123–133.
29. Krejci,L., Van Komen,S., Li,Y., Villemain,J., Reddy,M.S., Klein,H., Ellenberger,T. and Sung,P. (2003) DNA helicase Srs2 disrupts the Rad51 presynaptic filament. *Nature*, **423**, 305–309.
30. Veaute,X., Jeusset,J., Soustelle,C., Kowalczykowski,S.C., Le Cam,E. and Fabre,F. (2003) The Srs2 helicase prevents recombination by disrupting Rad51 nucleoprotein filaments. *Nature*, **423**, 309–312.
31. Miura,T., Shibata,T. and Kusano,K. (2013) Putative antirecombinase Srs2 DNA helicase promotes noncrossover homologous recombination avoiding loss of heterozygosity. *Proc. Natl. Acad. Sci. U.S.A.*, **110**, 16067–16072.
32. Kolesar,P., Altmannova,V., Silva,S., Lisby,M. and Krejci,L. (2016) Pro-recombination role of Srs2 requires SUMO but is independent of PCNA interaction. *J. Biol. Chem.*, **291**, 7594–7607.
33. Tran,H.T., Keen,J.D., Kricker,M., Resnick,M.A. and Gordenin,D.A. (1997) Hypermutability of homonucleotide runs in mismatch repair and DNA polymerase proofreading yeast mutants. *Mol. Cell. Biol.*, **17**, 2859–2865.
34. Lorenz,M.C., Muir,R.S., Lim,E., McElver,J., Weber,S.C. and Heitman,J. (1995) Gene disruption with PCR products in *Saccharomyces cerevisiae*. *Gene*, **158**, 113–117.
35. Nguyen,H.D., Becker,J., Thu,Y.M., Costanzo,M., Koch,E.N., Smith,S., Myung,K., Myers,C.L., Boone,C. and Bielinsky,A.-K. (2013) Unligated Okazaki fragments induce PCNA ubiquitination and a requirement for Rad59-dependent replication fork progression. *PLoS One*, **8**, e66379.
36. Clark,A.B., Cook,M.E., Tran,H.T., Gordenin,D.A., Resnick,M.A. and Kunkel,T.A. (1999) Functional analysis of human MutSα and MutSβ complexes in yeast. *Nucleic Acids Res.*, **27**, 736–742.
37. Becker,J.R., Nguyen,H.D., Wang,X. and Bielinsky,A.-K. (2014) Mcm10 deficiency causes defective-replisome-induced mutagenesis and a dependency on error-free postreplicative repair. *Cell Cycle*, **13**, 1737–1748.
38. Ricke,R.M. and Bielinsky,A.-K. (2006) A conserved Hsp10-like domain in Mcm10 is required to stabilize the catalytic subunit of DNA polymerase-α in budding yeast. *J. Biol. Chem.*, **281**, 18414–18425.
39. Zegerman,P. and Diffley,J.F. (2010) Checkpoint-dependent inhibition of DNA replication initiation by Sld3 and Dbf4 phosphorylation. *Nature*, **467**, 474–478.
40. Mann,H.B. and Whitney,D.R. (1947) On a test of whether one of two random variables is stochastically larger than the other. *Ann. Math. Stat.*, **18**, 50–60.
41. Drake,J.W. (1991) A constant rate of spontaneous mutation in DNA-based microbes. *Proc. Natl. Acad. Sci. U.S.A.*, **88**, 7160–7164.
42. Foster,P.L. (2006) Methods for determining spontaneous mutation rates. *Methods Enzymol.*, **409**, 195–213.
43. Gallo,D., Wang,G., Yip,C.M. and Brown,G.W. (2016) Analysis of replicating yeast chromosomes by DNA combing. *Cold Spring Harb. Protoc.*, **2016**, 138–149.
44. Motegi,A., Liaw,H.-J., Lee,K.-Y., Roest,H.P., Maas,A., Wu,X., Moinova,H., Markowitz,S.D., Ding,H. and Hoeijmakers,J.H. (2008) Polyubiquitination of proliferating cell nuclear antigen by HLTF and SHPRH prevents genomic instability from stalled replication forks. *Proc. Natl. Acad. Sci. U.S.A.*, **105**, 12411–12416.
45. Downs,J.A., Lowndes,N.F. and Jackson,S.P. (2000) A role for *Saccharomyces cerevisiae* histone H2A in DNA repair. *Nature*, **408**, 1001–1004.
46. Cobb,J.A., Schleker,T., Rojas,V., Bjergbaek,L., Tercero,J.A. and Gasser,S.M. (2005) Replisome instability, fork collapse, and gross chromosomal rearrangements arise synergistically from Mec1 kinase and RecQ helicase mutations. *Genes Dev.*, **19**, 3055–3069.
47. Balint,A., Kim,T., Gallo,D., Cussiol,J.R., de Oliveira,F.M.B., Yimit,A., Ou,J., Nakato,R., Gurevich,A. and Shirahige,K. (2015) Assembly of Slx4 signaling complexes behind DNA replication forks. *EMBO J.*, **34**, e201591190.
48. Osborn,A.J. and Elledge,S.J. (2003) Mrc1 is a replication fork component whose phosphorylation in response to DNA replication stress activates Rad53. *Genes Dev.*, **17**, 1755–1767.
49. Barford,J. and Hall,R. (1976) Estimation of the length of cell cycle phases from asynchronous cultures of *Saccharomyces cerevisiae*. *Exp. Cell Res.*, **102**, 276–284.
50. Stelter,P. and Ulrich,H.D. (2003) Control of spontaneous and damage-induced mutagenesis by SUMO and ubiquitin conjugation. *Nature*, **425**, 188–191.
51. Sacher,M., Pfander,B., Hoege,C. and Jentsch,S. (2006) Control of Rad52 recombination activity by double-strand break-induced SUMO modification. *Nat. Cell Biol.*, **8**, 1284–1290.
52. Cremona,C.A., Sarangi,P., Yang,Y., Hang,L.E., Rahman,S. and Zhao,X. (2012) Extensive DNA damage-induced sumoylation contributes to replication and repair and acts in addition to the mec1 checkpoint. *Mol. Cell*, **45**, 422–432.

53. Sartori,A.A., Lukas,C., Coates,J., Mistrik,M., Fu,S., Bartek,J., Baer,R., Lukas,J. and Jackson,S.P. (2007) Human CtIP promotes DNA end resection. *Nature*, **450**, 509–514.
54. Liu,S., Opiyo,S.O., Manthey,K., Glanzer,J.G., Ashley,A.K., Amerin,C., Troksa,K., Shrivastav,M., Nickoloff,J.A. and Oakley,G.G. (2012) Distinct roles for DNA-PK, ATM and ATR in RPA phosphorylation and checkpoint activation in response to replication stress. *Nucleic Acids Res.*, **40**, 10780–10794.
55. Rogakou,E.P., Pilch,D.R., Orr,A.H., Ivanova,V.S. and Bonner,W.M. (1998) DNA double-stranded breaks induce histone H2AX phosphorylation on serine 139. *J. Biol. Chem.*, **273**, 5858–5868.
56. Guo,Z., Kanjanapangka,J., Liu,N., Liu,S., Liu,C., Wu,Z., Wang,Y., Loh,T., Kowolik,C. and Jamsen,J. (2012) Sequential posttranslational modifications program FEN1 degradation during cell-cycle progression. *Mol. Cell*, **47**, 444–456.
57. Zhang,K., Keymeulen,S., Nelson,R., Tong,T.R., Yuan,Y.-C., Yun,X., Liu,Z., Lopez,J., Raz,D.J. and Kim,J.Y. (2018) Overexpression of flap endonuclease 1 correlates with enhanced proliferation and poor prognosis of Non–Small-Cell lung cancer. *Am. J. Pathol.*, **188**, 242–251.
58. He,L., Luo,L., Zhu,H., Yang,H., Zhang,Y., Wu,H., Sun,H., Jiang,F., Kathera,C.S. and Liu,L. (2017) FEN1 promotes tumor progression and confers cisplatin resistance in non-small-cell lung cancer. *Mol. Oncol.*, 640–654.
59. Sato,M., Girard,L., Sekine,I., Sunaga,N., Ramirez,R.D., Kamibayashi,C. and Minna,J.D. (2003) Increased expression and no mutation of the Flap endonuclease (FEN1) gene in human lung cancer. *Oncogene*, **22**, 7243–7246.
60. Yang,M., Guo,H., Wu,C., He,Y., Yu,D., Zhou,L., Wang,F., Xu,J., Tan,W. and Wang,G. (2009) Functional FEN1 polymorphisms are associated with DNA damage levels and lung cancer risk. *Hum. Mutat.*, **30**, 1320–1328.
61. Bakr,A., Oing,C., Köcher,S., Borgmann,K., Dornreiter,I., Petersen,C., Dikomey,E. and Mansour,W. (2015) Involvement of ATM in homologous recombination after end resection and RAD51 nucleofilament formation. *Nucleic Acids Res.*, **43**, 3154–3166.
62. Lee,S.E., Mitchell,R.A., Cheng,A. and Hendrickson,E.A. (1997) Evidence for DNA-PK-dependent and-independent DNA double-strand break repair pathways in mammalian cells as a function of the cell cycle. *Mol. Cell. Biol.*, **17**, 1425–1433.
63. Rajagopalan,P.R., Zhang,Z., McCourt,L., Dwyer,M., Benkovic,S.J. and Hammes,G.G. (2002) Interaction of dihydrofolate reductase with methotrexate: ensemble and single-molecule kinetics. *Proc. Natl. Acad. Sci. U.S.A.*, **99**, 13481–13486.
64. Jimeno,S., Herrera-Moyano,E., Ortega,P. and Aguilera,A. (2017) Differential effect of the overexpression of Rad2/XPG family endonucleases on genome integrity in yeast and human cells. *DNA Repair*, **57**, 66–75.
65. Jackson,S.P. and Durocher,D. (2013) Regulation of DNA damage responses by ubiquitin and SUMO. *Mol. Cell*, **49**, 795–807.
66. Waga,S., Hannon,G.J., Beach,D. and Stillman,B. (1994) The p21 inhibitor of cyclin-dependent kinases controls DNA replication by interaction with PCNA. *Nature*, **369**, 574–578.
67. Subramanian,J., Vijayakumar,S., Tomkinson,A.E. and Arnheim,N. (2005) Genetic instability induced by overexpression of DNA ligase I in budding yeast. *Genetics*, **171**, 427–441.
68. Li,X., Li,J., Harrington,J., Lieber,M.R. and Burgers,P.M. (1995) Lagging strand DNA synthesis at the eukaryotic replication fork involves binding and stimulation of FEN-1 by proliferating cell nuclear antigen. *J. Biol. Chem.*, **270**, 22109–22112.
69. Garg,P., Stith,C.M., Sabouri,N., Johansson,E. and Burgers,P.M. (2004) Idling by DNA polymerase δ maintains a ligatable nick during lagging-strand DNA replication. *Genes Dev.*, **18**, 2764–2773.
70. Ma,W., Resnick,M.A. and Gordenin,D.A. (2008) Apn1 and Apn2 endonucleases prevent accumulation of repair-associated DNA breaks in budding yeast as revealed by direct chromosomal analysis. *Nucleic Acids Res.*, **36**, 1836–1846.
71. Thandapani,P., Couturier,A.M., Yu,Z., Li,X., Couture,J.-F., Li,S., Masson,J.-Y. and Richard,S. (2017) Lysine methylation of FEN1 by SET7 is essential for its cellular response to replicative stress. *Oncotarget*, **8**, 64918–64931.
72. McManus,K.J., Barrett,I.J., Nouhi,Y. and Hieter,P. (2009) Specific synthetic lethal killing of RAD54B-deficient human colorectal cancer cells by FEN1 silencing. *Proc. Natl. Acad. Sci. U.S.A.*, **106**, 3276–3281.
73. van Pel,D.M., Barrett,I.J., Shimizu,Y., Sajesh,B.V., Guppy,B.J., Pfeifer,T., McManus,K.J. and Hieter,P. (2013) An evolutionarily conserved synthetic lethal interaction network identifies FEN1 as a broad-spectrum target for anticancer therapeutic development. *PLoS Genet.*, **9**, e1003254.
74. McWhirter,C., Tonge,M., Plant,H., Hardern,I., Nissink,W. and Durant,S.T. (2013) Development of a high-throughput fluorescence polarization DNA cleavage assay for the identification of FEN1 inhibitors. *J. Biomol. Screen.*, **18**, 567–575.